IRSTI 45.41.33, 50.43.17

**B. Sarsembayev**

*Nazarbayev University, Nur-Sultan, Kazakhstan*
***E-mail: bayandy_enu@mail.ru***

# Disturbance observer based discrete PI control system with back-calculation anti-windup technique for improvement transient performance of PMSM

**Abstract.** In this paper discrete-time field-oriented control (FOC) for PMSM speed control has been proposed. The cascade structure of the discrete-time PI-PI control system with tracking back-calculation anti-windup scheme. The novel anti-windup scheme for both loops has been adopted. Windup phenomena in traditional PI controllers have greater negative effects on the transient performance in engineering applications such as PMSM. In the real-time experiments, the proposed control system achieves less speed errors and faster response. The experimental results have proved the feasibility of the proposed control scheme.
**Key words:** PI controller, field-oriented control (FOC), permanent magnets synchronous motor (PMSM), back-calculation algorithm, discrete-time PI controller, anti-windup technique.

**DOI: doi.org/10.32523/2616-7263-2021-135-2-94-105**

## Introduction

Permanent magnet synchronous motors (PMSMs) have been utilized in the various applications. It is preferable due to its compact structures, high air-gap flux density, high power density, high torque to inertia ratio; higher efficiency than other electric motors [1].

Due to so-called windup phenomena in traditional PI, the controller's performance is not satisfactory for PMSM drives applications. This phenomena is characterized by long periods of overshoot, which results in poor control performance and even makes the overall system unstable. Therefore, modern PI-PI control system for motor drives are typically equipped with various anti-windup (AW) techniques to reduce integral effect on control system performance. The effectiveness of back-calculation based tracking gains AW scheme's performance has been experimentally demonstrated among other anti-windup techniques such as, simple limited integration, limited output with dead zone element, and conditioned integration with following applications such as angular position control of a servo system [2] and for PMSM control [3].

PI speed controller equipped with anti-windup scheme demonstrates good performance in both transient and steady-state times than with conventional forms [3]-[5]. However, PI controllers are sensitive to model uncertainty which is a case in practical applications[6]. In addition, the tuning gains of PI controller is tedious and time-consuming work. The defining of optimal gains for PI-PI control system based on analyzing plant's dynamics with step response method is most common among others [4].

In this paper cascade discrete PI-PI control has been utilized. While, the inner loop controls armature currents/torque whereas outer loop regulates the speed of motors by providing the current/torque reference [6].

Motivated by [3] in this study, PI-PI control scheme with novel anti-windup algorithm has been proposed for the PMSM speed regulation. The tracking back-calculation anti-windup scheme has been adopted and applied for both loops of the control system to compensate windup phenomena with aim of improving transient performance and achieving asymptotic stability of the closed-loop system. The discrete-time PI-PI control system are equipped with discrete-time tracking anti-windup scheme to handle windup phenomena.

### Surface mounted pmsm system

**A. Electrical subsystem model of pmsm**

The electrical model of the machine contains the equations for the stator current, stator flux and electromagnetic torque.

PMSM's stator d-q voltages are:

$$V_d = \frac{d\Psi_d}{dt} - \omega_{el}\Psi_q + R_s i_d \tag{1}$$

$$V_q = \frac{d\Psi_q}{dt} + \omega_{el}\Psi_d + R_s i_q \tag{2}$$

$\omega_{el}$ – electrical speed, rad/s

$i_q$ – q-axis current, A

$i_d$ – d –axis current, A

$\Psi_d$ and $\Psi_q$ - d-axis and q-axis magnetic flux linkages

$R_s$ – stator resistance, Ohm

$L_s$ – stator inductance, H

In the equations above it is the cross couplings of the two magnetic flux variables that stand out. Furthermore, the magnetic flux in the d- axis $\Psi_d$ acts positevely on the voltage $V_q$, and the magnetic flux in the q-axis $\Psi_q$ acts negatively on the voltage $V_d$.

The magnetic flux linkages are defined as

$$\Psi_d = L_d i_d + \lambda_m \tag{3}$$

$$\Psi_q = L_q i_q \tag{4}$$

$\lambda_m$– permanent magnet flux coefficient, Wb

The equation (3) demonstrates that the permanent flux is only aligned with the d-axis.

**B. Torque subsystem model of PMSM**

The voltages produced by $\omega_{el}\Psi_d$ and $-\omega_{el}\Psi_q$ corresponds to the back-emf in the system.

$$P_{el} = -\omega_{el}\Psi_q i_d + \omega_{el}\Psi_d i_q \tag{5}$$

Where the mechanical rotor shaft speed can be converted to electrical one through the expression

$$\omega_{el} = z_p\omega \tag{6}$$

$z_p$ – number of poles,

Taking into consideration that with $\Psi_d i_q$ and $\Psi_q i_d$ we are dealing with the peak value, it is then possible to compute the mechanical value of the active power using the following equation:

$$P_m = \frac{3}{2} z_p\omega(-\Psi_q i_d + \Psi_d i_q) \tag{7}$$

From definition of torque as related to power, the electromagnetic torque can be derived as

$$T_e = \frac{3}{2} z_p[(L_d - L_q) i_d i_q + \lambda_m i_q] \tag{8}$$

For the torque subsystem the following equations apply. The mechanical or produced torque considers losses due to friction, viscosity, and drag resulting from time-varying flux. The total torque, $T$ is difference between mechanical torque, $T_m$ (minus mechanical losses) and load torque, $T_L$.

Total torque is

$$T = T_m - T_L \tag{9}$$

$T_L$ – rated load torque, Nm

Mechanical torque is

$$T_m = T_e - T_{friction} - T_{viscous} - T_{d\Psi} \tag{10}$$

The torque losses due to friction is

$$T_{friction} = (C_{hy} + C_f)sign(\omega) \tag{11}$$

$C_f$ – static moment of friction, Nm

$C_{hy}$ – hysteresis losses coefficient, N·m

The torque losses due to viscousity is

$$T_{viscous} = (C_{ed} + d)\omega \tag{12}$$

The torque losses due to time-varying flux in the PMSM is

$$T_{d\Psi} = d_{ed}\frac{\frac{d\Psi_{dq}}{dt}\times\Psi_{dq}}{|\Psi_{dq}|^2} \tag{13}$$

$c_{ed}$ – eddy currents coefficient, Nm/(rad/s)

$d_{ed}$ – damping coefficient due to eddy currents Nm/(rad/s).

$d$ – viscous damping coefficient, Nm/(rad/s)

ω – mechanical speed, rad/s

$\Psi_{dq}$ – d-q frame magnetic flux linkage, Wb.

### C. Mechanical subsystem model of PMSM

Using equations (9) - (13) mechanical subsystem can be expressed as

$$T = J\frac{d\omega_m}{dt} \tag{14}$$

$J$ – rotor inertia, kg·cm²

From this mechanical speed of the rotor shaft of the PMSM system can be expressed as

$$\dot{\omega}_m = \frac{3}{2}\frac{z_p\lambda_m}{J}i_q - \frac{(C_{hy} + C_f)sign(\omega_m)}{J} - \frac{(C_{ed}+d)}{J}\omega_m - \frac{d_{ed}\frac{\frac{d\Psi_{dq}}{dt}\times\Psi_{dq}}{|\Psi_{dq}|^2}}{J} - \frac{T_L}{J} \tag{15}$$

$$y = \omega_m$$

The highly complex PMSM system should be controlled with sophisticated control system. The ordinary PI controller does not satisfy to the performance requirements in terms of overshoot and dynamic response due to so called windup phenomena.

In this control system, the time varying magnetic flux due to eddy currents, friction and hysteresis cause torque losses, which are also considered in the motion equation. The eddy currents are induced when a nonmagnetic, conductive material is moving in a magnetic field [7]–[9]. The eddy currents circulate in the rotor's conductive material and dissipate causing a repulsive force between the magnet and the conductor. Hence, the mechanical or produced torque considers losses due to static moment of friction, hysteresis, and time-varying flux.

## Control system design

### B. Discrete-time cascade pi-pi control system

For the speed regulation of the PMSM's parameters are not needed due to model free nature of PI control algorithm. Then PI-PI cascade closed-loop control is sufficient to achieve satisfactory performance for speed regulation (Figure 1). The control objective in this case is to achieve a specified tracking performance by means of the PI controller and facilitate zero errors in finite time.

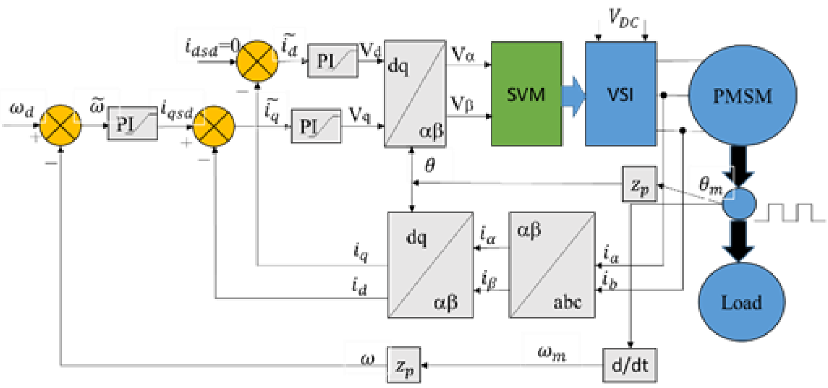


**Figure 1. Discrete-time cascade PI-PI control system for PMSM speed regulation**

The speed loop controller as well as currents controllers can be formulated with the following formulas based on Figure 2.

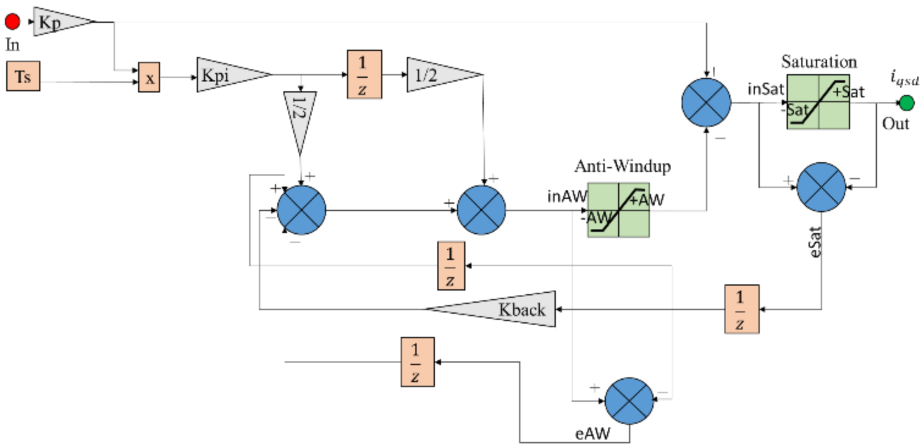


**Figure 2. Discrete-time PI controller with tracking anti-windup scheme**

$$|\mathrm{inSat} = 0|,\ \text{and}\ |\mathrm{inAW} = 0|\ \{\mathrm{out} = 0\} \tag{3}$$

$$|\mathrm{inSat} \geq \mp\mathrm{Sat}|,\ \text{and}\ |\mathrm{inAW} \geq \mp\mathrm{AW}|\ \{\mathrm{out} = \mp\mathrm{Sat}\} \tag{4}$$

$$|\mathrm{inSat} < \mp\mathrm{Sat}|\ \text{and}\ |\mathrm{inAW} \geq \mp\mathrm{AW}|, \\ \{\mathrm{out} = \tilde{\omega}\mathrm{K_p} - (\mp\mathrm{AW})\} \tag{5}$$

$$|\mathrm{inSat} < \mp\mathrm{Sat}| \text{and} |\mathrm{inAW} < \mathrm{AW}|,$$

$$\begin{cases} \mathrm{out} = \tilde{\omega}K_p - (\frac{1}{2}\frac{1}{z}K_{pi}\tilde{\omega}K_pT_s + (\frac{1}{2}K_{pi}\tilde{\omega}K_pT_s + \\ \frac{1}{z}\mathrm{inAW} - \frac{1}{z}\mathrm{eSat}K_{back} - \frac{1}{z}\mathrm{eAW})) \end{cases} \quad (6)$$

where

inSat – input of saturation block
∓Sat – output of saturation block
out – output of PI controller
inAW – input of anti-windup block
∓AW – output of anti-windup block
eSat – error of saturation block
eAW – error of anti-windup block
$\tilde{\omega}$ – speed error, RPM
$K_p$ – proportional gain
$K_{pi}$ – proportional-integral gain
$T_s$ – sampling time
$\frac{1}{z}$ – unit delay
$K_{back}$ – back-calculation gain

**Experimental results**

For the experimental setup DSP based "Controlled permanent magnet servo drive with MATLAB/Simulink 300W" (manufactured by Lucas-Nuelle gGmbH) was used to test the proposed PI-PI control system with tracking anti-windup scheme. The experimental setup comprises surface mounted type PMSM that coupled with 1024 pulses incremental position encoder and servo-machine operated with ActiveServo software acting as a load. The control algorithm is written in Matlab/Simulink (R2016b) environment then the code generated by Code Composed Studio 5 is sent to servo-converter for real-time experiment control. Note, after loading the code, no modification of gains is allowed. For a new configuration and modification of gains, the code generation has to be performed again. The switching period of the self-commutated converter is set to 125 μs. The control routine frequency for the pulse width modulation technique (PWM) in the inverter is set to 8 kHz. The parameters of the PMSM are listed in Table 1.

To confirm the effectiveness of the proposed control system design, let us consider a prototype of SPMSM with the following nominal parameters given in Table 1.

**Table 1**

**PMSM nominal parameters**

| Motor parameters | Symbol | Value |
|---|---|---|
| Rated speed | $n_n$ (RPM) | 6000 |
| Rated torque | $M_n$ (Nm) | 0.97 |
| Rated power | $P_n$ (W) | 300 |
| Torque constant | $K_{tRMS}$ (Nm/A) | 0.41 |
| Voltage constant | $K_{eRMS}$ (Nm/A) | 26.1 |
| Permanent magnetic flux coefficient | $\lambda_m$ (Vs) | 0.089 |

| | | |
|---|---|---|
| Winding resistance Ph-Ph | $R_s$ (Ohm) | 4.74 |
| Winding inductance Ph-Ph | $L_s$ (mH) | 8.6 |
| Rotor's moment of inertia | $J$ (kgcm²) | 0.33 |
| Number of poles | $z_p$ | 8 |
| Static moment of friction | $C_f$ (Nm) | 0.014 |
| Hysteresis losses coefficient | $C_{hys}$ (Nm) | 0.08 |
| Viscous damping coefficient | b (N·m/(rad/s)) | 0.002 |
| Eddy currents coefficient | $c_{ed}$ (Nm/(rad/s)) | 0.0015 |
| Eddy currents damping coefficient | $d_{ed}$ (Nm/(rad/s)) | 0.003 |

A space vector pulse width modulation (SVPWM) technique is used to regulate the phase currents flowing into the PMSM. For evaluation of performance of the proposed control scheme, in this paper, the experimental results of the baseline controller without HODO are compared with the results of the proposed HODO based PI-PI control system with tracking anti-windup scheme utilized. Two cases with speed variation and load torque disturbance have been investigated.

**Table 2**

**Control system's parameters**

| Controllers and Observers | Parameters and Gains |
|---|---|
| Speed controller PI gains | $K_p = 0.057, K_I = 0.04$ |
| Current controllers PI gains | $K_p = 17.1, K_I = 0.0018$ |

*Case 1:* Speed Transient Response with nominal parameters
1) The desired speed ($\omega_d$): 300 RPM $\rightarrow$ 600 RPM.
2) Constant load torque $T_L = 0.5$ Nm.
3) No load torque disturbance.
*Case 2:* Load Torque Transient Response
1) The desired speed $\omega_d = 500$ RPM.
2) Load torque disturbance $T_L = 0.3$ Nm $\rightarrow$ 0.5 Nm.

The round or trapezoidal shaped reference speed has been chosen for PMSM, as it is more effective against wear of mechanical coupling of the prototype PMSM like in the industrial applications [10]. However, the load torque disturbance has been applied as step-wise.

Traditional discrete-time PI controller has been equipped with tracking back-calculation anti-windup scheme to improve transient performance PMSM system. The speed response and the references currents have been plotted for graphical evaluation purposes.

Figs. 3-8 show the experimental results of the proposed control method under two operational cases to assess its performance . The currents and the voltages have been measured and converted to d-q frame ($i_{qs}, i_{ds}, V_{qs}, V_{ds}$). The mechanical speed of PMSM ($\omega$) as well as its tracking error ($\tilde{\omega}$) have been shown and compared with their reference values. Figures 3, 4, and 5 are results under conditions in *Case 1*, while Figures 6, 7, and 8 are results obtained under operation conditions in *Case 2*. The detailed performance of the proposed control design is summarized in Table 3. The experimental results shown below are assessed by the maximum angular shaft speed errors, settling time and absolute mean mechanical speed error. The maximum angular shaft speed errors are 42 and 17 RPM for *Case 1* and *Case 2* respectively. While the settling time 0.3 and 0.17 seconds, the absolute mean mechanical speed errors are 1.4838% and 0.172% respectively. The control inputs $V_{qs}$ and $V_{ds}$ under operational conditions in *Case 1* and *Case 2* have been demonstrated in Figures 5 and 8.

**Table 3**

**Performance of the proposed discrete-time PI-PI with tracking back-calculation anti-windup control scheme for both loops**

| Criteria and cases | | PI with anti-windup |
|---|---|---|
| Maximum angular shaft speed error, RPM | Case 1 | 42 |
| | Case 2 | 17 |
| Settling time, s | Case 1 | 0.3 |
| | Case 2 | 0.17 |
| Absolute mean of the mechanical speed error,% | Case 1 | 1.4838% |
| | Case 2 | 0.172% |

In the PMSM system, the pulsating torques can be seen in the d-q currents plots as well as they are reflected in PMSM angular shaft speed response. The origin of these ripples may come from cogging torques associated with the shape of th rotor of the machine, but also high-frequency electromagnetic noise associated with switching time periods in the power converter. The minimizing the current ripples in the PMSM prototyping kit will be sought in future research.

a)

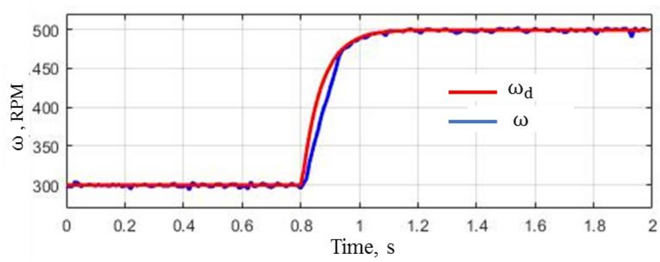

b)

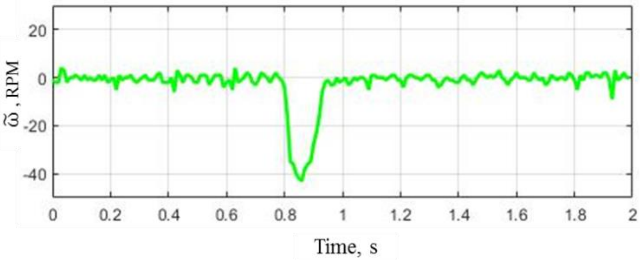


**Figure 3. Experimental results of the proposed control for Case 1. (a) Mechanical speed response of PMSM; (b) Mechanical speed errors.**

a)

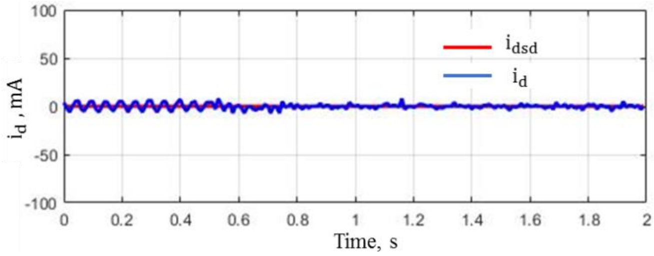


b)

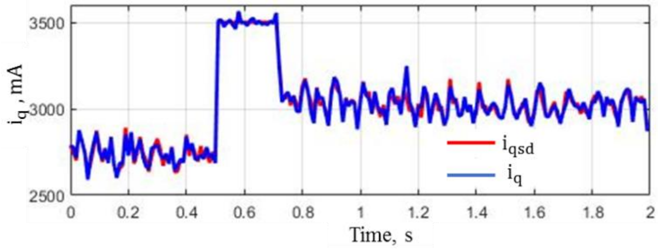


**Figure 4. dq-axis currents of the proposed control for case 1. (a) $i_{ds}$ and its desired value $i_{dsd}$; (b) $i_{qs}$ and its desired value $i_{qsd}$.**

a)

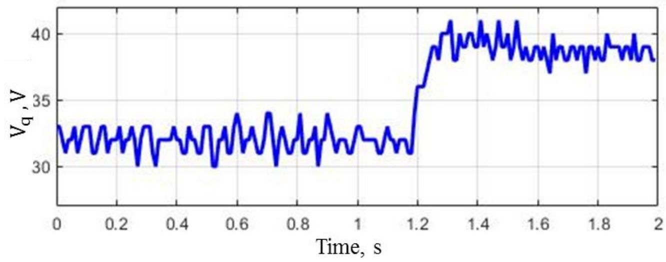


b)

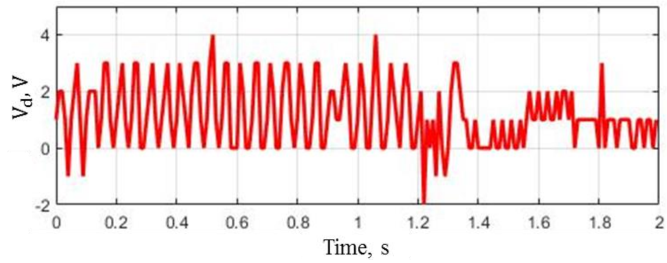


**Figure 5. dq-axis voltages of the proposed control for Case 1. (a) control input on q-axis $V_{qs}$; (b) control input on d-axis $V_{ds}$.**

a)

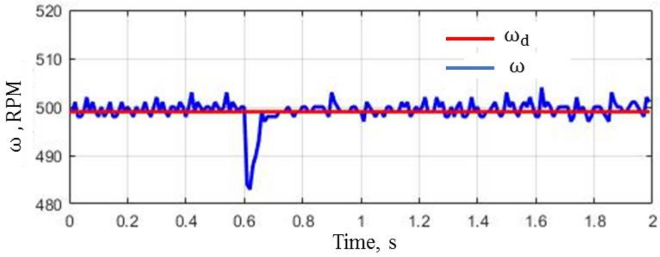


b)

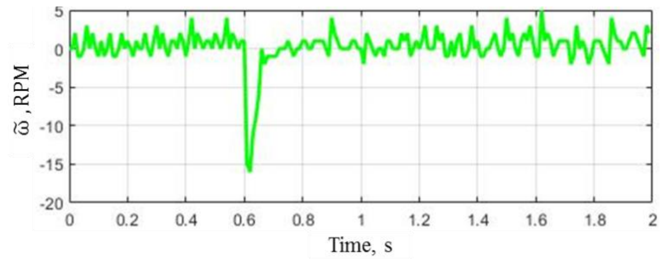


**Figure 6. Experimental results of the proposed control for Case 2. (a) Mechanical speed response of PMSM; (b) Mechanical speed error.**

a)

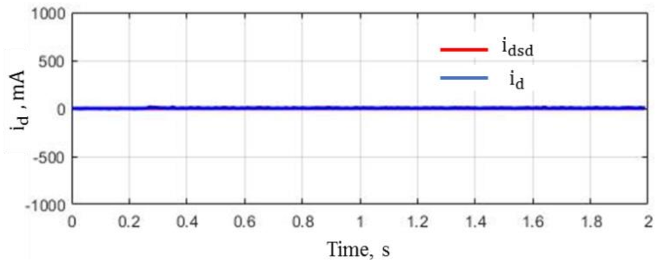


b)

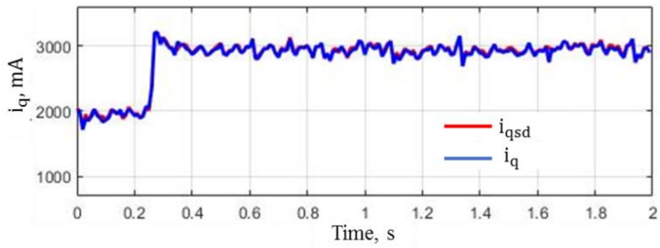


**Figure 7. dq- axis currents of the proposed control for Case 2. (a) $i_{ds}$ and its desired value $i_{dsd}$; (b) $i_{qs}$ and its desired value $i_{qsd}$.**

a)

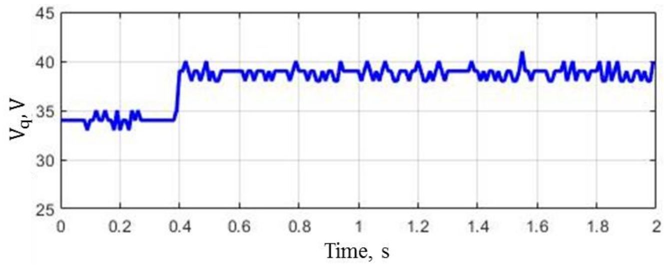

b)

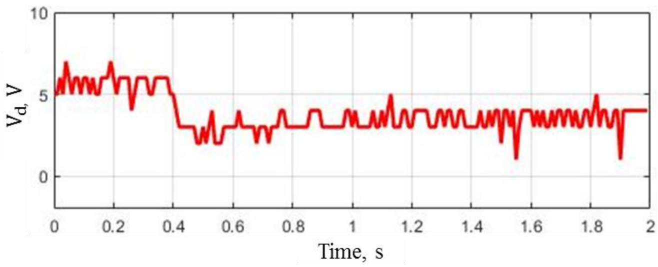


**Figure 8. dq- axis voltages of the prposed control for Case 2. (a) control input on q-axis $V_{qs}$; (b) control input on d-axis $V_{ds}$.**

## Conclusion

In this paper, field-oriented control based discrete-time PI-PI with tracking back-calculation anti-windup scheme is proposed. The cascade discrete-time PI-PI control structure with novel anti-windup scheme has been adopted for both loops. Unlike traditional PI controllers, the proposed controller can significantly improve the performance of PMSM system under speed and load torque variations. As the currents ripples are unavoidable, their reduction will be considered in future works.

## References

1. T.D. Do, H.H. Choi, and J.-W. Jung, "Nonlinear Optimal DTC Design and Stability Analysis for Interior Permanent Magnet Synchronous Motor Drives," *IEEE/ASME Trans. Mechatronics*, -2015. -vol. 20, no. 6. -pp. 2716-2725.

2. R.E. Precup, R. C. David, E. M. Petriu, M. B. Radac, and S. Preitl, "Adaptive GSA-based optimal tuning of PI controlled servo systems with reduced process parametric sensitivity, robust stability and controller robustness," *IEEE Trans. Cybern.* -2014. -vol. 44, no. 11. -pp. 2168-2267.

3. J. Espina, A. Arias, J. Balcells, C. Ortega, and S. Galceran, "Speed anti-windup PI strategies review for field oriented control of permanent magnet synchronous machines servo drives with matrix converters," in *13th European Conference on Power Electronics and Applications*, Barcelona, Spain, -2009. -pp. 279-285.

4. K.J. Astrom and T. Hagglung, *Advanced PID Control*. NC, USA: ISA, -2006.

5. Y. Zhetpissov, A. Kaibaldiyev, and T. D. Do, "PI anti-windup speed control of permanent magnet synchronous motor based on feedforward compensation," 2018 ELEKTRO, Mikulov, Czech Rep., -2018, -pp. 1-8, doi: 10.1109/ELEKTRO.2018.8398275.

6. R. Errouissi, A. Al-Durra, and S. M. Muyeen, "Experimental Validation of a Novel PI Speed Controller for AC Motor Drives with Improved Transient Performances," IEEE Trans. Control Syst. Technol. -2018. -vol. 26, no. 4. -pp. 1414-1421.

7. J. Bae, J. Hwang, J. Park, and D. Kwag, "Modeling and experiments on eddy current damping caused by a permanent magnet in a conductive tube," *J. Mech. Sci. Technol.* -2009. -vol. 23. -pp. 3024-3035.

8. H.A. Sodano and J. Bae, "Eddy Current Damping in Structures," *Shock Vib. Dig.* -2004. -vol. 36, no. 6. -pp. 469–478.

9. Abdullah, J.-H. Ahn, and H.-Y. Kim, "Effect of Electromagnetic Damping on System

Performance of Voice-Coil Actuator Applied to Balancing-Type Scale," Actuators. -2020. -vol. 9, no. 8. -pp. 1-23.

10. S. Li, J. Yang, W.-H. Chen, and C. Xisong, *Disturbance observer-based control: methods and applications*. Boca Raton-London-New York: CRC Press, -2014.

**Б. Сарсембаев**

*Назарбаев Университеті, Нұр-Сұлтан, Қазақстан*

**ТМСЭҚ-нің өнімділігін жақсарту үшін контроллердің ауытқуға қарсы кері есептеу алгоритмі қолданған кедергілерді бақылаушыға негізделген дискретті PI басқару жүйесі**

**Аңдатпа.** Бұл жұмыста турақты магнитті синхронды электр қозғалтқыш (ТМСЭҚ) жылдамдығын басқаруға арналған дискретті уақыттық өрістік бағдарлау басқарудың (ӨББ) негізінде ұсынылды. Қайта есептелетін ауытқуға қарсы схемасы бар дискретті уақытты ПИ-ПИ басқару жүйесінің каскадты құрылымы қолданды. Екі шенбер үшін де ауытқуға қарсы жаңа схема қабылданды. Дәстүрлі ПИ контроллерлеріндегі өтпелі құбылыстары ТМСЭҚ сияқты инженерлік шешімдерде өтпелі жұмысына үлкен теріс әсер етеді. Нақты уақыттағы эксперименттерде ұсынылған басқару жүйесі аз қателікке және жылдам жауап беруге қол жеткізеді. Тәжірибе нәтижелері ұсынылған бақылау схемасының орындылығын дәлелдеді.

**Түйін сөздер:** тұрақты магниттер синхронды электр қозғалтқыш (ТМСЭҚ), кері есептеу алгоритмі, PI дискретті контроллер.

**Б. Сарсембаев**

*Назарбаев Университет, Нур-Султан, Казахстан*

**Дискретная система ПИ-регулирования с техникой обратного вычисления на основе наблюдателя возмущений для улучшения переходных характеристик в СЭПМ**

**Аннотация.** В этой статье было предложено управление с дискретным временем, ориентированное на поле (УОП) для управления скоростью СЭПМ. Каскадная структура системы управления PI-PI с дискретным временем и схемой анти-вихревание с отслеживанием обратных вычислений. Была принята новая схема предотвращения закручивания для обоих контуров. Явление закрутки в традиционных контроллерах PI имеет большее отрицательное влияние на переходные характеристики в инженерных приложениях, таких как СЭПМ. В экспериментах в режиме реального времени предлагаемая система управления обеспечивает меньшее количество ошибок скорости и более быструю реакцию. Результаты экспериментов подтвердили реализуемость предложенной схемы управления.

**Ключевые слова:** синхронный электродвигатель с постоянными магнитами (СЭПМ), алгоритм обратного вычисления, дискретный ПИ-регулятор.

**References**

1. T. D. Do, H. H. Choi, and J.-W. Jung, "Nonlinear Optimal DTC Design and Stability Analysis for Interior Permanent Magnet Synchronous Motor Drives," *IEEE/ASME Trans. Mechatronics*, vol. 20, no. 6, pp. 2716–2725, 2015.

2. R. E. Precup, R. C. David, E. M. Petriu, M. B. Radac, and S. Preitl, "Adaptive GSA-based optimal tuning of PI controlled servo systems with reduced process parametric sensitivity, robust stability and controller robustness," *IEEE Trans. Cybern.*, vol. 44, no. 11, pp. 2168-2267, 2014.

3. J. Espina, A. Arias, J. Balcells, C. Ortega, and S. Galceran, "Speed anti-windup PI strategies review for field oriented control of permanent magnet synchronous machines servo drives with matrix converters," in *13th European Conference on Power Electronics and Applications*, Barcelona, Spain, 2009, pp. 279–285.

4. K. J. Astrom and T. Hagglung, *Advanced PID Control*. NC, USA: ISA, 2006.

5. Y. Zhetpissov, A. Kaibaldiyev, and T. D. Do, "PI anti-windup speed control of permanent magnet synchronous motor based on feedforward compensation," 2018 ELEKTRO, Mikulov, Czech Rep., 2018, pp. 1-8, doi: 10.1109/ELEKTRO.2018.8398275.

6. R. Errouissi, A. Al-Durra, and S. M. Muyeen, "Experimental Validation of a Novel PI Speed Controller for AC Motor Drives with Improved Transient Performances," *IEEE Trans. Control Syst. Technol.*, vol. 26, no. 4, pp. 1414–1421, 2018.

7. Bae, J. Hwang, J. Park, and D. Kwag, "Modeling and experiments on eddy current damping caused by a permanent magnet in a conductive tube," *J. Mech. Sci. Technol.*, vol. 23, pp. 3024–3035, 2009.

8. H. A. Sodano and J. Bae, "Eddy Current Damping in Structures," *Shock Vib. Dig.*, vol. 36, no. 6, pp. 469-478, 2004.

9. Abdullah, J.-H. Ahn, and H.-Y. Kim, "Effect of Electromagnetic Damping on System Performance of Voice-Coil Actuator Applied to Balancing-Type Scale," *Actuators*, vol. 9, no. 8, pp. 1-23, 2020.

10. S. Li, J. Yang, W.-H. Chen, and C. Xisong, *Disturbance observer-based control: methods and applications*. Boca Raton-London-New York: CRC Press, 2014.

**Information about authors:**

*B. Sarsembayev* - Department of Robotics, School of Engineering and Digital Sciences (SEDS), Nazarbayev University, Nur-Sultan Z05H0P9, Kazakhstan

*Б. Сарсембаев* - Робототехника бөлімі, Инженерлік және цифрлық ғылымдар мектебі (SEDS), Назарбаев Университеті, Нұр-Сұлтан Z05H0P9, Қазақстан.